10.1161/CIRCULATIONAHA.119.041059

HHIPL1, a Gene at the 14q32 Coronary Artery Disease Locus, Positively Regulates Hedgehog Signaling and Promotes Atherosclerosis

Running Title: *Aravani et al.; HHIPL1 Promotes Atherosclerosis*

Dimitra Aravani, PhD[1]; Gavin E. Morris, PhD[1]; Peter D. Jones, PhD[1]; Helena K. Tattersall, MSc[1]; Elisavet Karamanavi, PhD[1]; Michael A. Kaiser, BSc[1]; Renata B. Kostogrys, PhD[2]; Maryam Ghaderi Najafabadi, MSc[1]; Sarah L. Andrews, MSc[1]; Mintu Nath, PhD[1]; Shu Ye, MD, PhD[1]; Emma J. Stringer, PhD[1]; Nilesh J. Samani, MD[1]; Tom R. Webb, PhD[1]

[1]Department of Cardiovascular Sciences, University of Leicester and National Institute for Health Research Leicester Biomedical Research Centre, Leicester, United Kingdom, Glenfield Hospital, Leicester, LE3 9QP, UK; [2]Department of Human Nutrition, Faculty of Food Technology, University of Agriculture in Kraków, ul. Balicka 122, 30-149 Kraków, Poland

Address for Correspondence:
Tom R. Webb, PhD
Department of Cardiovascular Sciences
University of Leicester
Cardiovascular Research Centre
Glenfield Hospital, Leicester, LE3 9QP, UK
Tel: +44 116 204 4762
Email: tw126@le.ac.uk

Abstract

Background: Genome-wide association studies have identified chromosome 14q32 as a locus for coronary artery disease. The disease associated variants fall in a hitherto uncharacterised gene called *Hedgehog Interacting Protein Like 1 (HHIPL1)*, which encodes a sequence homologue of an antagonist of hedgehog signaling. The function of HHIPL1 and its role in atherosclerosis is unknown.

Methods: HHIPL1 cellular localization, interaction with Sonic Hedgehog (SHH) and influence on hedgehog signaling were tested. *HHIPL1* expression was measured in coronary artery disease relevant human cells and protein localization was assessed in wild-type and *Apoe*$^{-/-}$ mice. Human aortic smooth muscle cell phenotypes and hedgehog signaling were investigated following gene knockdown. *Hhipl1*$^{-/-}$ mice were generated and aortic smooth muscle cells collected for phenotypic analysis and assessment of hedgehog signaling activity. *Hhipl1*$^{-/-}$ mice were bred onto both the *Apoe*$^{-/-}$ and *Ldlr*$^{-/-}$ knockout strains and the extent of atherosclerosis was quantified following 12 weeks of high fat diet. Cellular composition and collagen content of aortic plaques was assessed by immunohistochemistry.

Results: *In vitro* analyses revealed that HHIPL1 is a secreted protein that interacts with SHH and increases hedgehog signaling activity. *HHIPL1* expression was detected in human smooth muscle cells and in smooth muscle within atherosclerotic plaques of *Apoe*$^{-/-}$ mice. The expression of *Hhipl1* increased with disease progression in aortic roots of *Apoe*$^{-/-}$ mice. Proliferation and migration was reduced in *Hhipl1* knockout mouse and *HHIPL1* knockdown aortic smooth muscle cells and hedgehog signaling was decreased in *HHIPL1* deficient cells. *Hhipl1* knockout caused a reduction of more than 50% in atherosclerosis burden on both *Apoe*$^{-/-}$ and *Ldlr*$^{-/-}$ knockout backgrounds and lesions were characterized by reduced smooth muscle cell content.

Conclusions: HHIPL1 is a secreted proatherogenic protein that enhances hedgehog signaling and regulates smooth muscle cell proliferation and migration. Inhibition of HHIPL1 protein function might offer a novel therapeutic strategy for coronary artery disease.

Key Words: Coronary artery disease; Atherosclerosis; Genome wide association; Hedgehog signaling

Clinical Perspective

What is new?

- This is the first investigation of HHIPL1, a candidate gene at the chromosome 14q32 coronary artery disease locus identified through genome-wide association studies.
- We show that HHIPL1 is a secreted protein that interacts with Sonic Hedgehog and is a positive regulator of hedgehog signaling.
- In murine models, HHIPL1 deficiency attenuates the development of atherosclerosis by reducing smooth muscle cell proliferation and migration.

What are the clinical implications?

- Our study supports HHIPL1 as the causal gene at the 14q32 coronary artery disease locus.
- HHIPL1 is a promising therapeutic target that affects a pathogenic mechanism not addressed by current treatments for coronary artery disease.

Introduction

Over the last decade, genome-wide association studies (GWAS) have identified a large number of loci that associate with increased risk of coronary artery disease (CAD) [1–4]. Remarkably, only around one third are also associated with conventional cardiovascular risk factors [2] and many loci contain genes that have not previously been implicated in cardiovascular pathophysiology [3]. Investigation of the function of these genes and identifying the pathways through which the genetic variants exert their effects might facilitate the development of novel therapeutic strategies for the treatment of CAD.

The CAD associated variants at the 14q32 locus fall in *Hedgehog Interacting Protein Like 1* (*HHIPL1*), a gene of unknown function that encodes a paralogue of the hedgehog signaling regulator Hedgehog Interacting Protein (HHIP) [5,6].

The mammalian hedgehog proteins (Sonic Hedgehog (SHH), Desert Hedgehog (DHH) and Indian Hedgehog (IHH)) are secreted molecules that exert a concentration and time dependent effect on target cells [7]. Signal transduction is initiated upon binding of a hedgehog ligand to the canonical receptor Patched (PTCH1 and 2) [8], leading to disinhibition of Smoothened (SMO). SMO triggers a complex signaling cascade regulating the activation of GLI family zinc finger transcription factors (GLI1, 2 and 3) [7]. GLI activators induce the transcription of target genes primarily involved in cell proliferation, cell survival and cell fate specification. Among those genes are several components of the hedgehog pathway itself, including PTCH and GLI [9,10]. HHIP modulates hedgehog signaling activity by binding and inhibiting the action of hedgehog proteins [5,6,11,12]. Hedgehog signaling is indispensable for normal embryonic development [7] and plays critical roles in the maintenance of adult progenitor and stem cell populations and in tissue repair following injury [13]. In the cardiovascular system, hedgehog signaling is essential for early vascular development [14–16], vascular remodelling in the yolk sac [17,18] arterial-venous

identity [19,20], development and maintenance of the coronary vasculature [20,21] and vessel maturation [22]. In adults, hedgehog signaling is involved in the maintenance of adult vasculature and for ischemia-induced neovascularization, including after myocardial infarction [23–27]. The role of hedgehog signaling in atherosclerosis is less well defined. Expression of hedgehog pathway components has been detected in plaques and inhibition of hedgehog signaling using an antibody that blocks binding of all three hedgehog proteins to PTCH1 increased atherosclerosis in *Apoe*$^{-/-}$ mice [28,29].

Here, we report the first experimental investigation of HHIPL1 and present evidence that it is a secreted proatherogenic protein which regulates smooth muscle cell proliferation and migration.

Methods

Upon reasonable request, the data, analytic methods, and study materials will be made available to other researchers for the purposes of reproducing the results. Extended methods are provided in the Supplemental Methods section in the Data Supplement.

Reagents and cell-lines

Plasmids were prepared by the Protein Expression Laboratory (PROTEX) cloning service at the University of Leicester. Immunoprecipitation was performed using GFP-TRAP beads (Chromotek). anti-FLAG (F3165, Sigma), anti-GFP (MA5-15256 ThermoFisher Scientific), anti-GLI1 (AF3455, R&D Systems) and anti-β-actin (11355703, ThermoFisher Scientific) were used for immunoblotting. HEK293 cells were purchased from ATCC, human aortic smooth muscle cells (AoSMCs) from Invitrogen and ThermoFisher Scientific, peripheral blood mononuclear cells (PBMCs) and macrophages were prepared as described previously [30]. Coronary artery endothelial cells (CAECs) were purchased from Promocell. SHH-LIGHT2 cells were the kind gift of Professor PA Beachy, Stanford University.

SHH reporter assays

Analysis of hedgehog signaling activity was performed using SHH-LIGHT2 cells, a clonal NIH-3T3 cell line stably expressing a Gli-dependent firefly luciferase and constitutive *Renilla* reporters, as previously described [31] with minor modifications. SHH-LIGHT2 cells were seeded in 96-well plates at a density of 4,000 cells per well in 200 µl DMEM with 10% FBS. Once confluent, cells were cultured for a further 12 to 24 hours before treatment with conditioned media. Conditioned media was prepared by transfecting HEK293 cells with SHH-GFP, HHIP-FLAG, HHIPL1-GFP or GFP control plasmid. 24-hours post-transfection, media was changed to DMEM with 0.5% FBS and collected after a further 24 hours for treatment of SHH-LIGHT2 cells. Firefly luciferase and *Renilla* was measured 24 hours post-treatment using the Dual-Glo Luciferase assay system (Promega) and read on a Novostar plate reader (BMG LabTech). The hedgehog signaling activity of mouse AoSMCs was measured by co-culturing wild-type or *Hhipl1* $^{-/-}$ cells with SHH-LIGHT2 cells. Three wild-type and three *Hhipl1*$^{-/-}$ AoSMCs were used for experiments. Cells were seeded at 5,000 SHH-LIGHT2 and 2,500 AoSMCS per well in 96-well plates in replicates of 3 to 6. When cells reached confluency media was changed to DMEM containing 0.5% FBS. Luciferase activity was measured 24 hours later.

Cellular assays

Proliferation was determined by incubating with PrestoBlue® (ThermoFisher Scientific) and measuring fluorescence emission or by counting cells. Cell migration was measured using a wound-healing assay. Apoptosis was measured by staining cells with FITC-Annexin-V (Biolegend) and measured using a Beckman Coulter Gallios flow cytometer.

Generation of mouse models

All work involving animals was approved by the local animal ethical committee and performed according to ARRIVE guidelines and under United Kingdom Home Office Project

Licence (60/4332). All mice were housed in an SPF facility in an IVC system, were group housed wherever possible and the health status checked routinely. Other than weight gain associated with high fat diet, no mice demonstrated any adverse effects. A genetically altered mouse strain was generated from embryonic stem (ES) cells (*Hhipl1*$^{tm1a(KOMP)Wtsi}$), purchased from The Knock Out Mouse Project (KOMP), by the Gene Editing and Archiving Service (GenEAS) in the University of Leicester Division of Biological Services. All work reported here has been carried out on mice carrying the knock out first allele (*Hhipl1*$^{tm1a(KOMP)Wtsi}$), which is subsequently referred to as *Hhipl1*$^{-/-}$.

Analysis of atherosclerosis

The *Hhipl1*$^{-/-}$ strain was backcrossed onto C57BL6/J background for 6 generations before being intercrossed with *Apoe*$^{-/-}$ and *Ldlr*$^{-/-}$ mice to generate *Hhipl1* $^{-/-}$*;Apoe*$^{-/-}$ and *Hhipl1* $^{-/-}$*;Ldlr*$^{-/-}$ mice and control littermates. Due to genotype requirements mice could not be randomized into groups. Experiments were powered for *en face* analysis of atherosclerosis as the primary objective. The intercrossed mice were fed a high fat 'western' diet (TestDiet® 5TJN: fat 40%, carbohydrate 44%, protein 16%, cholesterol 0.15%) for 12 weeks from 6 weeks of age. The aortic roots and thoracic aortas were collected and processed. For *en face* analysis, following overnight fixation in 4% PFA the thoracic aorta was opened longitudinally and stained with 60 % Oil Red O (Sigma-Aldrich) and imaged using a DM2500 Leica microscope. The lipid stained area was quantified using LAS V 4.0 software by a researcher blinded to genotype and is presented as a percentage of total aortic area. For aortic roots, lesion area was measured on Oil Red O stained sections from frozen embedded hearts. Ninety 10 μm sections were collected to obtain 900 μm of aortic length from the appearance of the aortic sinus (identified by the appearance of aortic cusps), which was deemed point zero. Quantification of lesion area was performed across nine sections (100 μm

between sections). For *en face* analysis the data is presented as average lesion area normalized to total aorta area. For aortic root analysis the data is presented as area.

Atherosclerotic lesion compositional analysis

Smooth muscle cells were stained using anti-α-SMA (Abcam ab5694), which detects smooth muscle alpha-actin 2 (ACTA2), and macrophages were stained using Macrophages/Monocytes antibody (MOMA-2) (BIORAD MCA519G). Slides were fixed in cold acetone at -20^{o}C, air dried, and endogenous peroxidase activity was blocked in 0.3% H_2O_2/Methanol. Non-specific binding was reduced by incubation in 2.5% goat serum (Vector Laboratories) before primary antibody incubation at 4 ^{o}C in a humidified chamber overnight. Slides were incubated with ImmPRESS HRP anti-Rabbit (Vector Laboratories, MP-7451) or anti-Rat IgG Peroxidase (Vector Laboratories, MP-7444) and staining was visualised using DAB and counterstained in haematoxylin (Gill No. 2, Sigma Aldrich). Images were acquired using a DM2500 Leica microscope. Positively stained areas of each aorta were measured using ImageJ by a researcher blinded to genotype. The data is presented as the average of positively stained lesion areas (9 serial sections) normalised by total lesion area. For collagen and lipid core quantification, sections were stained with Masson's Trichrome (Sigma-Aldrich) according to the manufacturer's instructions.

Hhipl1 staining

Serial frozen aortic root sections from *Apoe*$^{-/-}$ as well as from wild type mice were stained by IHC with anti-HHIPL1 (HPA052767, Atlas Antibodies), MOMA-2 (BIORAD MCA519G) and SMA (ab32575, Abcam) antibodies using the same methodology as before. Immunofluorescence was performed on paraffin-embedded aortic root sections from *Apoe*$^{-/-}$ mice, using anti-HHIPL1 antibody and Cy3-conjugated mouse monoclonal anti–α-SMA (1:200 C6198, Sigma-Aldrich) antibodies. Sections were treated with antigen unmasking solution (H-3301, Vector Laboratories). Alexa Fluor 488–labelled goat anti-mouse secondary

antibody (ThermoFisher) was used to detect anti-HHIPL1 antibody localization. Images were acquired using a DM2500 Leica fluorescent microscope. Dual staining was quantified across three sections using ImageJ.

Statistical analysis

Results are presented as mean ± standard deviation unless stated otherwise. We conducted two-sample unpaired t-tests for the variables that were normally distributed and compared between two groups. If the variable was not normally distributed we carried out a Mann-Whitney test. For the SHH reporter, *Hhipl1* expression and human AoSMC migration data we employed the analysis of variance (ANOVA) approach to compare more than two groups. For mouse and human AoSMC proliferation data, the ANOVA model also incorporated time and two-way interaction effect of group and time. We modelled the body weight of each mouse (measured separately at weekly intervals through the study) using a linear mixed model, incorporating genotype and time as fixed effects and mouse as a random effect. We assessed all models for underlying assumptions using appropriate plots and statistics. When multiple comparisons of grouping variables were conducted, we adjusted estimated probabilities by Tukey's method to account for multiple comparisons. All statistical tests were two-sided with type 1 error rate (p-value) of 0.05 to determine statistical significance. All statistical analyses were carried out using the GraphPad Prism 7.00 (GraphPad software Inc.) and R software version 3.5 (R Core Team, 2018).

Results

HHIPL1 is a secreted positive regulator of SHH

HHIPL1 encodes a predicted secreted protein consisting of an N-terminal signal peptide followed by a span of 550 amino acids that shares approximately 50% identity to the hedgehog interacting region of HHIP and a C-terminal scavenger receptor cysteine rich

(SRCR) domain. We assessed the localization of the HHIPL1 protein by expressing C-terminally FLAG GFP-tagged HHIPL1 expression constructs (HHIPL1-FLAG and HHIPL1-GFP) in HEK293 cells. We detected HHIPL1-FLAG by western blotting in both HEK293 cell lysates and in conditioned media precipitated with trichloroacetic acid (**Figure 1A**). No HHIPL1-GFP was seen at the cell surface suggesting that HHIPL1 is not associated with the cell membrane (**Figure 1B and 1C).**

Next, we investigated whether HHIPL1 interacts with SHH, the best characterised ligand of the hedgehog pathway. HEK293 cells were co-transfected by electroporation with HHIPL1-FLAG and SHH-GFP plasmids or empty vector controls followed by immunoprecipitation with GFP-trap beads. Both HHIPL1-FLAG and SHH-GFP fusion proteins were detected in the immunoprecipitated samples indicating that HHIPL1 and SHH interact (**Figure 1D**).

To assess whether HHIPL1 modulates SHH signaling we performed reporter assays using SHH-LIGHT2 cells [30]. HHIPL1-GFP in conditioned medium significantly increased Gli-luciferase activity compared to SHH-GFP alone (P<0.001) (**Figure 1E**), suggesting HHIPL1 acts as a positive regulator of SHH. HHIP-FLAG caused a non-significant reduction compared to SHH-GFP treatment (P=0.44).

HHIPL1 is expressed by smooth muscle cells **and controls cell proliferation and migration**

We measured *HHIPL1* in primary human AoSMCs, CAECs, PBMCs and macrophages and found highest expression in AoSMCs (**Figure 2A**). In addition, the Human Protein Atlas identified high levels of HHIPL1 protein in human smooth muscle cells and breast myoepithelial cells as well as lower levels in cardiac and skeletal muscle myocytes. [32]. We used siRNA knockdown to investigate the cellular consequences of *HHIPL1* deficiency in human AoSMCs. We used two siRNAs to reduce *HHIPL1* expression and achieved

knockdown efficiencies between 70% and 95% compared to a non-targeting control siRNA (NTC) (**Figure 2B**). Knockdown was retained over a period of 72 hours. We performed a scratch assay to assess the effect of *HHIPL1* deficiency on human AoSMC migration and found that the migration rate of *HHIPL1* knockdown AoSMCs was lower than NTC transfected cells (siRNA1 $P<0.001$, siRNA2 $P<0.001$) (**Figure 2C**). We assessed the proliferation of *HHIPL1* knockdown cells using a fluorescent cell viability assay and observed a reduction in cell number in *HHIPL1* knockdown cells compared to controls (siRNA1 $P=0.02$, siRNA2 $P=0.03$ at 72 hours) (**Figure 2D**). We detected no difference in apoptosis between control and *HHIPL1* knockdown cells (**Figure 2E**).

GLI1 expression is reduced in HHIPL1 deficient aortic smooth muscle cells

Hedgehog signaling activates gene expression of pathway members including *GLI1* and *PTCH1*. We measured the expression of both genes following *HHIPL1* knockdown in human AoSMCs and detected a significant reduction in *GLI1* expression (siRNA1 $P=0.041$, siRNA2 $P=0.0002$) (**Figure 2F**). We confirmed the reduction in GLI1 protein expression by western blotting (Figure 2G). We did not detect a difference in *PTCH1* expression. We also assessed *PTCH2* expression, but this was below the threshold for quantification.

***Hhipl1 is present in smooth muscle cells in vivo and its* expression increases in atherosclerosis**

We investigated the expression of *Hhipl1* in a hyperlipidemic mouse atherosclerosis model. First, we performed immunohistochemical analysis to detect Hhipl1 protein in aortic root sections from 18 week old *Apoe*$^{-/-}$ mice fed a high fat western diet. Hhipl1 expression most closely matched cells stained with the smooth muscle marker ACTA2, but not those stained with MOMA-2, which recognises a mouse macrophage antigen (**Figure 3A and Figure S1A**). We also detected Hhipl1 expression in aortic arches from wild-type mice (**Figure S1B**).

We performed immunofluorescence staining of plaques to confirm expression of Hhipl1 in smooth muscle cells (**Figure 3B**) and detected Hhipl1 expression in 93.7% ± 2.6% cells (n=3) of ACTA2 expressing cells.

Next, we assessed *Hhipl1* levels during atherosclerosis progression by measuring its expression in RNA collected from the aortic arch of *Apoe*$^{-/-}$ mice between 6 and 48 weeks of age. *Hhipl1* expression increased by approximately three-fold through the study (**Figure 3C**). Post-hoc comparisons to the 6-week time-point showed a significant increase in expression at 32 (P=0.002), 40 (P<0.001) and 48 weeks (P<0.001). *Hhipl1* expression did not change in the aortic arch of wild-type mice across the same timeframe (**Figure S1C**) indicating that the increase in expression was the result of disease rather than age.

Generation and characterisation of *Hhipl1* knockout mice

We obtained mouse ES cells carrying the Hhipl1 tm1a knockout first allele, which consists of a reporter-tagged insertion into intron 1 of the *Hhipl1* gene (**Figure S2A**) from the KOMP repository and generated *Hhipl1*$^{-/-}$ mice. The gene-trap is predicted to cause a truncated Hhipl1 protein of just 91 amino acids. We confirmed absence of *Hhipl1* expression in *Hhipl1*$^{-/-}$ mice at the mRNA level by RT-PCR (**Figure S2B**). *Hhipl1*$^{-/-}$ mice were monitored for signs of sub-viability and dysmorphology at all stages, but nothing of note was observed. Mice were born in the expected Mendelian frequency and there were no losses peri or postnatally. Animals were weighed weekly and showed no difference in weight in comparison to wild-type littermates.

***Hhipl1* knockout aortic smooth muscle cells show reduced proliferation and migration**

We collected AoSMCs from knockout mice and wild-type littermates to test the effect of *Hhipl1* deficiency on cell phenotype. Migration (P=0.02) (**Figure 4A**) and proliferation (**Figure 4B**) (P<0.001 at 96 hours culture) of *Hhipl1*$^{-/-}$ mouse AoSMCs was decreased compared to wild-type cells. We saw no difference in apoptosis between groups (**Figure 4C**).

***Hhipl1* knockout aortic smooth muscle cells have reduced hedgehog signaling activity**

To investigate hedgehog signaling activity we cultured wild-type and *Hhipl1*$^{-/-}$ mouse AoSMCs together with SHH-LIGHT2 cells and performed luciferase reporter assays. Gli-luciferase activity was significantly reduced in knockout cells (P=0.008) **(Figure 4D**). Similar to our experiments in human cells, we detected a reduction in expression of the hedgehog target gene *Gli1* at both the mRNA (P=0.02) and protein level (**Figure 4E and 4F**). We did not detect a change in *Ptch1* expression in *Hhipl1*$^{-/-}$ AoSMCs.

***Hhipl1* knockout decreases atherosclerosis in two mouse models**

We investigated the effect of *Hhipl1* knockout on atherosclerosis in both *Apoe*$^{-/-}$ and *Ldlr*$^{-/-}$ mice. Male double knockouts (*Hhipl1*$^{-/-}$; *Apoe*$^{-/-}$ and *Hhipl1*$^{-/-}$; *Ldlr*$^{-/-}$) were fed a Western diet for 12 weeks and compared to littermates wild-type for *Hhipl1* (*Hhipl1*$^{+/+}$; *Apoe*$^{-/-}$ and *Hhipl1*$^{+/+}$; *Ldlr*$^{-/-}$). Atherosclerosis was quantified in the aorta by *en face* (n=18-19 per group) and in sections of the aortic root (n=6-10 per group). *Hhipl1*$^{-/-}$*; Ldlr*$^{-/-}$ mice exhibited a reduction of 56% in lesion area (7.5% (95% CI 6.3%, 8.7%)) compared to *Hhipl1*$^{+/+}$*; Ldlr*$^{-/-}$ littermate controls (3.3% (95% CI 2.3%, 4.4%) as measured by *en face* (P=5x10^{-6}) (**Figure 5A and 5B**). In aortic roots there was a 37% reduction in mean lesion area between *Hhipl1*$^{+/+}$*; Ldlr*$^{-/-}$ (3.08x10^5 μm^2 (95% CI 2.37x10^5, 3.79x10^5 μm2)) and *Hhipl1*$^{-/-}$*; Ldlr*$^{-/-}$ (1.93x10^5 μm^2 (95% CI 1.25x10^5, 2.61x10^5 μm^2)) mice (P=0.013) (**Figure 5C and 5D**). Similarly, *Hhipl1*$^{-/-}$; *Apoe*$^{-/-}$ mice displayed a 53% reduction in lesion area (7.5% (95% CI 5.7%, 9.2%)) compared to *Hhipl1*$^{+/+}$; *Apoe*$^{-/-}$ controls (3.5% (95% CI 2.5%, 4.4%)) by *en face* (P=0.0002) (**Figure 5E and 5F**). Aortic roots from *Hhipl1*$^{-/-}$; *Apoe*$^{-/-}$ mice showed a decrease of 33% in mean lesion area (3.84x10^5 μm^2 (95% CI 2.92x10^5, 4.76x10^5 μm^2)) versus (2.57x10^5 μm^2 (95% CI 1.97x10^5, 3.16x10^5 μm^2)) compared to controls (P=0.039) (**Figure 5G and 5H**).

There was no difference in body weight, plasma lipid levels or blood pressure between experimental and control groups on either background (**Figure S3A-S3F**).

***Hhipl1* knockout reduces smooth muscle cell content in mouse atherosclerotic plaques**

We characterized the cellular and collagen composition of aortic root lesions from *Hhipl1*$^{-/-}$; *Ldlr*$^{-/-}$ (**Figure 6A-6H**) and *Hhipl1*$^{-/-}$; *Apoe*$^{-/-}$ mice (**Figure 7A-7H**) compared to *Hhipl1* wild-type littermates. Image analysis for lesion component coverage (as a percentage of the total lesion area) revealed no difference in lipids or macrophages within plaques of *Hhipl1*$^{-/-}$; *Ldlr*$^{-/-}$ mice compared to controls (**Figure 6A-6D**). We detected a 46% reduction in cells stained for SMA in *Hhipl1*$^{-/-}$; *Ldlr*$^{-/-}$ lesions (13.9% (95% CI 9.7%, 18.2%)) compared to controls (25.6% (95% CI 20.9%, 30.5%)) (*P*=0.004) (**Figure 6E and 6F**) as well as a non-significant reduction in collagen content *Hhipl1*$^{-/-}$; *Ldlr*$^{-/-}$ (*P*=0.07) (**Figure 6G and 6H**). We did detect a reduction in the lipid content of *Hhipl1*$^{-/-}$; *Apoe*$^{-/-}$ plaques (28.5% (95% CI 26%, 31%)) compared to controls (32.9% (95% CI 29.6%, 36.2%)) (*P*=0.02) (**Figure 7A and 7B**). The other components of *Apoe*$^{-/-}$ plaques showed similar differences to those observed on the *Ldlr*$^{-/-}$ background. There was no difference in macrophage staining (Figure 7C and 7D), a 47% reduction in SMA positive staining in *Hhipl1*$^{-/-}$; *Apoe*$^{-/-}$ mice (15.3% (95% CI 9.3%, 21.4%)) compared to controls (29.1% (95% CI 24.2%, 33.9%)) (*P*=0.001) (**Figure 7E and 7F**) and a non-significant decrease in collagen content (*P*=0.08) (**Figure 7G and 7H**). In addition to higher smooth muscle and collagen content, *Hhipl1*$^{+/+}$ mice plaques from *Hhipl1*$^{-/-}$ mice contained fewer cholesterol crystals and smaller lipid cores than controls (**Figure S4A-S4F**).

Discussion

A major challenge post-GWAS is the identification of the causal gene and biological mechanisms underlying each disease-associated locus. In this study, we investigated

HHIPL1, an uncharacterised gene at the chromosome 14q32 CAD locus and showed that it encodes a secreted SHH regulator that modulates atherosclerosis relevant smooth muscle cell phenotypes. We detected Hhipl1 expression in smooth muscle cells in atherosclerotic plaques and its expression increased with disease progression. Most strikingly, knockout of *Hhipl1* caused a substantial decrease in atherosclerosis on two different disease prone backgrounds. Our data strongly support *HHIPL1* as the causal gene at the 14q32 CAD locus, links hedgehog signaling to atherosclerosis and identifies HHIPL1 as a potential target for therapeutic intervention.

HHIPL1 is a paralogue of the hedgehog signaling modulator HHIP [5], which interacts with each of the three hedgehog ligands and inhibits signaling [6,11,12]. HHIP is associated with lung function and chronic obstructive pulmonary disease in humans [33,34] and homozygous knockout of *Hhip* in mice causes lethality due to abnormal lung development [35], while heterozygous knockout animals develop emphysema [36]. The function of HHIPL1 has not previously been investigated. Our data demonstrate that HHIPL1, like HHIP, is a secreted hedgehog interacting protein; however, unlike HHIP, HHIPL1 positively regulates hedgehog signaling. In addition to its homology with HHIP, HHIPL1 also contains a C-terminal SRCR domain. This domain is present in some of the scavenger receptors involved in lipid uptake in plaque development and is thought to be involved protein-protein interactions or ligand binding [37]. Interestingly, cholesterol modification of the hedgehog proteins controls their distribution and receptor interactions [38]. It is unclear whether the HHIPL1 SRCR is involved in the interaction with SHH via its cholesterol modification or some other mechanism, or if it is required for a different hedgehog independent function.

We detected *HHIPL1* expression in AoSMCs and found that HHIPL1 protein localized to smooth muscle cells in atherosclerotic plaques. We also observed increased

Hhipl1 expression in the aortic roots of older *Apoe*$^{-/-}$ mice. This is likely to be the result of increased numbers of smooth muscle cells during atherosclerosis progression; however, we cannot exclude *Hhipl1* expression also being affected by other factors related to plaque development. In normal adult arteries, the core hedgehog proteins are expressed between the adventitial and medial layers [39] and following injury in smooth muscle cells in the media and intima [40,41]. Whilst our results suggest that smooth muscle is the primary site of HHIPL1 function, we cannot exclude a role for Hhipl1 in other atherosclerosis relevant cell-types, such as endothelial or inflammatory cells. Conditional knockout of Hhipl1 in smooth muscle will help determine the cell-specificity of its role in disease pathogenesis.

HHIPL1 deficiency reduced smooth muscle cell migration and proliferation in both human and mouse cells *in vitro*, and reduced the proportion of smooth muscle cells in plaques *in vivo*. The hedgehog signaling pathway is an established regulator of cell behaviour in multiple different systems [7,42,43], including smooth muscle cells [22,40,41,44–46]. Hedgehog proteins can control these phenotypes through a variety of different mechanisms including directly acting as chemoattractants and by inducing signalling pathways involved in cell-shape regulation and cell-cycle control. Although the exact mechanism of action of the hedgehog pathway on smooth muscle is unclear, SHH has been shown to mediate PDGFB induced smooth muscle migration via ERK and PI3K signalling [22] and hedgehog induction of neuropilins, which act as co-receptors of semaphorins and VEGF, has been linked to cell migration in the development of the aortic arch [46]. Previous studies have also demonstrated that inhibition of hedgehog signalling induces smooth muscle cell apoptosis [45,47]. We did not detect a difference in apoptosis in either our mouse or human experiments, which is possibly a result of the moderate reduction in hedgehog signaling caused by *HHIPL1* deficiency compared to substantial loss of activity through pathway inhibition.

Our data clearly demonstrate a role for *HHIPL1* in atherosclerosis with *Hhipl1* knockout reducing plaque burden by more than 50% in two different hyperlipidemic mouse models. This reduction was not due to any changes in body weight, blood or plasma lipids. Previously, Beckers *et al*. used a monoclonal antibody that inhibits all three hedgehog proteins to investigate atherosclerosis in *Apoe*$^{-/-}$ mice and found that treated animals had larger more advanced atherosclerotic plaques [29]. The findings of this study are somewhat different to ours as *Apoe*$^{-/-}$ mice treated with the inhibitory antibody did not gain weight, had reduced plasma cholesterol levels, and the increase in atherosclerosis was driven by an in increase in macrophage content with no effect on smooth muscle. The efficiency of hedgehog inhibition in cells in the vessel wall was minimal and the differences with our study probably reflect the more general effects of global hedgehog inhibition. Nevertheless, both data support a role for hedgehog signaling in atherosclerosis and further investigation of the hedgehog pathway in disease pathogenesis and as a potential target for the treatment of CAD is warranted. Our data would suggest that inhibition of hedgehog signalling would reduce plaque development and several hedgehog pathway inhibitors exist including the smoothened antagonists vismodegib and sonidegib, which have FDA approval for treatment of basal cell carcinoma [49,50]. Directly targeting HHIPL1 might also represent a promising option for therapy.

Current drug therapies for reducing atherosclerosis are primarily targeted toward lipids. Our findings suggest that targeting vascular smooth muscle cells may also be beneficial. Smooth muscle cell proliferation also plays a role in other vascular pathologies including restenosis following percutaneous coronary intervention and coronary graft occlusion. Whether HHIPL1 plays a role in these conditions and targeting it would be of benefit remains to be determined.

In conclusion, HHIPL1, whose locus is associated with CAD in humans, is a new positive regulator of hedgehog signaling that promotes atherosclerosis in mice. Known hedgehog pathway modulators or novel therapeutics that directly target HHIPL1 are potential new treatments for CAD.

Acknowledgments

We acknowledge the staff in the University of Leicester Division of Biomedical Services for technical expertise and animal care and the University of Leicester Core Biotechnology Services for assistance in plasmid construction (PROTEX) and image analysis (Advanced Imaging Facility). We thank Professor PA Beachy for providing the SHH-LIGHT2 cell line We thank Professor Martin Bennett for providing sections from *Apoe*$^{-/-}$ mice.

Author Contributions:

D.A., N.J.S., E.J.S., and T.R.W. designed the study. D.A., G.E.M., P.D.J., and H.K.T. performed experiments. E.K., and R.B.K. contributed to immunohistochemical analysis. M.A.K., M.N.G., and S.L.A contributed to cell-based experiments. D.A., and M.N. performed statistical analyses. Data analysis and interpretation was performed by D.A., G.E.M., P.D.J., H.K.T., M.N., S.Y., N.J.S., E.J.S., and T.R.W. All authors contributed to the writing and preparation of the manuscript.

Sources of Funding

The research leading to these results has received funding from the European Union Seventh Framework Programme FP7/2007-2013 under grant agreement number HEALTH-F2-2013-601456, a Transatlantic Networks of Excellence Award (12CVD02) from The Leducq Foundation and the British Heart Foundation (SP/18/8/33620) as a partner of the European Research Area Network on Cardiovascular Diseases (ERA-CVD) druggable-MI-genes

(01KL1802) and supported by the UK National Institute for Health Research (NIHR) Leicester Biomedical Research Centre. NJS is a UK NIHR Senior Investigator. G.E.M, S.Y and T.R.W are funded by the British Heart Foundation (SP/16/4/32697).

Disclosures

None

References

1. Schunkert H, König IR, Kathiresan S, Reilly MP, Assimes TL, Holm H, Preuss M, Stewart AF, Barbalic M, Gieger C, Absher D, Aherrahrou Z, Allayee H, Altshuler D, Anand SS, Andersen K, Anderson JL, Ardissino D, Ball SG, Balmforth AJ, Barnes TA, Becker DM, Becker LC, Berger K, Bis JC, Boekholdt SM, Boerwinkle E, Braund PS, Brown MJ, Burnett MS, Buysschaert I; Cardiogenics, Carlquist JF, Chen L, Cichon S, Codd V, Davies RW, Dedoussis G, Dehghan A, Demissie S, Devaney JM, Diemert P, Do R, Doering A, Eifert S, Mokhtari NE, Ellis SG, Elosua R, Engert JC, Epstein SE, de Faire U, Fischer M, Folsom AR, Freyer J, Gigante B, Girelli D, Gretarsdottir S, Gudnason V, Gulcher JR, Halperin E, Hammond N, Hazen SL, Hofman A, Horne BD, Illig T, Iribarren C, Jones GT, Jukema JW, Kaiser MA, Kaplan LM, Kastelein JJ, Khaw KT, Knowles JW, Kolovou G, Kong A, Laaksonen R, Lambrechts D, Leander K, Lettre G, Li M, Lieb W, Loley C, Lotery AJ, Mannucci PM, Maouche S, Martinelli N, McKeown PP, Meisinger C, Meitinger T, Melander O, Merlini PA, Mooser V, Morgan T, Mühleisen TW, Muhlestein JB, Münzel T, Musunuru K, Nahrstaedt J, Nelson CP, Nöthen MM, Olivieri O, Patel RS, Patterson CC, Peters A, Peyvandi F, Qu L, Quyyumi AA, Rader DJ, Rallidis LS, Rice C, Rosendaal FR, Rubin D, Salomaa V, Sampietro ML, Sandhu MS, Schadt E, Schäfer A, Schillert A, Schreiber S, Schrezenmeir J, Schwartz SM, Siscovick DS, Sivananthan M, Sivapalaratnam S, Smith A, Smith TB, Snoep JD, Soranzo N, Spertus JA, Stark K, Stirrups K, Stoll M, Tang WH, Tennstedt S, Thorgeirsson G, Thorleifsson G, Tomaszewski M, Uitterlinden AG, van Rij AM, Voight BF, Wareham NJ, Wells GA, Wichmann HE, Wild PS, Willenborg C, Witteman JC, Wright BJ, Ye S, Zeller T, Ziegler A, Cambien F, Goodall AH, Cupples LA, Quertermous T, März W, Hengstenberg C, Blankenberg S, Ouwehand WH, Hall AS, Deloukas P, Thompson JR, Stefansson K, Roberts R, Thorsteinsdottir U, O'Donnell CJ, McPherson R, Erdmann J; CARDIoGRAM Consortium, Samani NJ.Large-scale association analysis identifies 13 new susceptibility loci for coronary artery disease. *Nat Genet*. 2011;43:333–338. doi:10.1038/ng.784.
2. Nikpay M, Goel A, Won HH, Hall LM, Willenborg C, Kanoni S, Saleheen D, Kyriakou T, Nelson CP, Hopewell JC, Webb TR, Zeng L, Dehghan A, Alver M, Armasu SM, Auro K, Bjonnes A, Chasman DI, Chen S, Ford I, Franceschini N, Gieger C, Grace C, Gustafsson S, Huang J, Hwang SJ, Kim YK, Kleber ME, Lau KW, Lu X, Lu Y, Lyytikäinen LP, Mihailov E, Morrison AC, Pervjakova N, Qu L, Rose LM, Salfati E, Saxena R, Scholz M, Smith AV, Tikkanen E, Uitterlinden A, Yang X, Zhang W, Zhao W, de Andrade M, de Vries PS, van Zuydam NR, Anand SS, Bertram L, Beutner F,

Dedoussis G, Frossard P, Gauguier D, Goodall AH, Gottesman O, Haber M, Han BG, Huang J, Jalilzadeh S, Kessler T, König IR, Lannfelt L, Lieb W, Lind L, Lindgren CM, Lokki ML, Magnusson PK, Mallick NH, Mehra N, Meitinger T, Memon FU, Morris AP, Nieminen MS, Pedersen NL, Peters A, Rallidis LS, Rasheed A, Samuel M, Shah SH, Sinisalo J, Stirrups KE, Trompet S, Wang L, Zaman KS, Ardissino D, Boerwinkle E, Borecki IB, Bottinger EP, Buring JE, Chambers JC, Collins R, Cupples LA, Danesh J, Demuth I, Elosua R, Epstein SE, Esko T, Feitosa MF, Franco OH, Franzosi MG, Granger CB, Gu D, Gudnason V, Hall AS, Hamsten A, Harris TB, Hazen SL, Hengstenberg C, Hofman A, Ingelsson E, Iribarren C, Jukema JW, Karhunen PJ, Kim BJ, Kooner JS, Kullo IJ, Lehtimäki T, Loos RJ, Melander O, Metspalu A, März W, Palmer CN, Perola M, Quertermous T, Rader DJ, Ridker PM, Ripatti S, Roberts R, Salomaa V, Sanghera DK, Schwartz SM, Seedorf U, Stewart AF, Stott DJ, Thiery J, Zalloua PA, O'Donnell CJ, Reilly MP, Assimes TL, Thompson JR, Erdmann J, Clarke R, Watkins H, Kathiresan S, McPherson R, Deloukas P, Schunkert H, Samani NJ, Farrall M. A comprehensive 1,000 Genomes-based genome-wide association meta-analysis of coronary artery disease. *Nat Genet*. 2015;47:1121–1130. doi:10.1038/ng.3396.

3. Klarin D, Zhu QM, Emdin CA, Chaffin M, Horner S, McMillan BJ, Leed A, Weale ME, Spencer CCA, Aguet F, Segrè AV, Ardlie KG, Khera AV, Kaushik VK, Natarajan P, CARDIoGRAMplusC4D Consortium, Kathiresan S. Genetic analysis in UK Biobank links insulin resistance and transendothelial migration pathways to coronary artery disease. *Nat Genet*. 2017;49:1392–1397. doi:10.1038/ng.3914.
4. Nelson CP, Goel A, Butterworth AS, Kanoni S, Webb TR, Marouli E, Zeng L, Ntalla I, Lai FY, Hopewell JC, Giannakopoulou O, Jiang T, Hamby SE, Di Angelantonio E, Assimes TL, Bottinger EP, Chambers JC, Clarke R, Palmer CNA, Cubbon RM, Ellinor P, Ermel R, Evangelou E, Franks PW, Grace C, Gu D, Hingorani AD, Howson JMM, Ingelsson E, Kastrati A, Kessler T, Kyriakou T, Lehtimäki T, Lu X, Lu Y, März W, McPherson R, Metspalu A, Pujades-Rodriguez M, Ruusalepp A, Schadt EE, Schmidt AF, Sweeting MJ, Zalloua PA, AlGhalayini K, Keavney BD, Kooner JS, Loos RJF, Patel RS, Rutter MK, Tomaszewski M, Tzoulaki I, Zeggini E, Erdmann J, Dedoussis G, Björkegren JLM; EPIC-CVD Consortium; CARDIoGRAMplusC4D; UK Biobank CardioMetabolic Consortium CHD working group, Schunkert H, Farrall M, Danesh J, Samani NJ, Watkins H, Deloukas P. Association analyses based on false discovery rate implicate new loci for coronary artery disease. *Nat Genet.* 2017;49:1385–1391. doi:10.1038/ng.3913.
5. Katoh Y, Katoh M. Comparative genomics on HHIP family orthologs. *Int J Mol Med* 2006;17:391-395.
6. Chuang PT, McMahon AP. Vertebrate Hedgehog signalling modulated by induction of a Hedgehog-binding protein. *Nature*. 1999;397:617–621.
7. Ingham PW, McMahon AP. Hedgehog signaling in animal development: paradigms and principles. *Genes Dev*. 2001;15:3059–3087.
8. Marigo V, Davey RA, Zuo Y, Cunningham JM, Tabin CJ. Biochemical evidence that Patched is the Hedgehog receptor. *Nature*. 1996;384:176-179.
9. Marigo V, Tabin CJ. Regulation of patched by sonic hedgehog in the developing neural tube. *Proc Natl Acad Sci USA*. 1996;93:9346-9351.
10. Marigo V, Johnson RL, Vortkamp A, Tabin CJ. Sonic hedgehog Differentially Regulates Expression of GLI and GLI3 during Limb Development. *Dev Biol*. 1996;180:273–283.

11. Kwong L, Bijlsma MF, Roelink H. Shh-mediated degradation of Hhip allows cell autonomous and non-cell autonomous Shh signalling. *Nat Commun.* 2014;5:4849. doi:10.1038/ncomms5849.
12. Holtz AM, Griffiths SC, Davis SJ, Bishop B, Siebold C, Allen BL. Secreted HHIP1 interacts with heparan sulfate and regulates Hedgehog ligand localization and function. *J Cell Biol*. 2015;209:739–758.
13. Petrova R, Joyner AL. Roles for Hedgehog signaling in adult organ homeostasis and repair. *Development*. 2014;141:3445-3457. doi:10.1242/dev.083691.
14. Dyer MA, Farrington SM, Mohn D, Munday JR, Baron MH. Indian hedgehog activates hematopoiesis and vasculogenesis and can respecify prospective neurectodermal cell fate in the mouse embryo. *Development.* 2001;128:1717–1730.
15. Vokes SA, Yatskievych TA, Heimark RL, McMahon J, McMahon AP, Antin PB, Krieg PA. Hedgehog signaling is essential for endothelial tube formation during vasculogenesis. *Development.* 2004;131:4371–4380.
16. Coultas L, Nieuwenhuis E, Anderson GA, Cabezas J, Nagy A, Henkelman RM, Hui CC, Rossant J. Hedgehog regulates distinct vascular patterning events through VEGF-dependent and -independent mechanisms. *Blood.* 2010;116:653–660. doi:10.1182/blood-2009-12-256644.
17. Nagase M, Nagase T, Koshima I, Fujita T. Critical time window of hedgehog-dependent angiogenesis in murine yolk sac. *Microvasc Research*. 2006;71:85–90.
18. Byrd N, Becker S, Maye P, Narasimhaiah R, St-Jacques B, Zhang X, Mcmahon J, Mcmahon A, Grabel L. Hedgehog is required for murine yolk sac angiogenesis. *Development.* 2002;129:361–372.
19. Lawson ND, Scheer N, Pham VN, Kim CH, Chitnis AB, Campos-Ortega JA, Weinstein BM. Notch signaling is required for arterial-venous differentiation during embryonic vascular development. *Development*. 2001;128:3675–3683.
20. Lavine KJ, Long F, Choi K, Smith C, Ornitz DM. Hedgehog signaling to distinct cell types differentially regulates coronary artery and vein development. *Development.* 2008;135:3161–3171. doi:10.1242/dev.019919.
21. Lavine KJ, White AC, Park C, Smith CS, Choi K, Long F, Hui C, Ornitz DM. Fibroblast growth factor signals regulate a wave of Hedgehog activation that is essential for coronary vascular development. *Genes Dev*. 2006;20:1651–1666.
22. Yao Q, Renault MA, Chapouly C, Vandierdonck S, Belloc I, Jaspard-Vinassa B, Daniel-Lamaziere JM, Laffargue M, Merched A, Desgranges C, Gadeau AP. Sonic hedgehog mediates a novel pathway of PDGF-BB-dependent vessel maturation. *Blood.* 2014;123:2429–2437. doi:10.1182/blood-2013-06-508689.
23. Lavine KJ, Kovacs A, Ornitz DM. Hedgehog signaling is critical for maintenance of the adult coronary vasculature in mice. *J Clin Invest.* 2008;118:2404–2414. doi:10.1172/JCI34561.
24. Pola R, Losordo DW, Ling LE, Aprahamian TR, Barban E, Bosch-Marce M, Curry C, Corbley M, Kearney M, Isner JM. Postnatal recapitulation of embryonic hedgehog pathway in response to skeletal muscle ischemia. *Circulation*. 2003;108:479–485.
25. Kusano KF, Pola R, Murayama T, Curry C, Kawamoto A, Iwakura A, Shintani S, Ii M, Asai J, Tkebuchava T, Thorne T, Takenaka H, Aikawa R, Goukassian D, von Samson P, Hamada H, Yoon YS, Silver M, Eaton E, Ma H, Heyd L, Kearney M, Munger W, Porter JA, Kishore R, Losordo DW. Sonic hedgehog myocardial gene therapy: tissue repair through transient reconstitution of embryonic signaling. *Nat Med*. 2005;11:1197–1204.
26. Pola R, Ling LE, Silver M, Corbley MJ, Kearney M, Blake Pepinsky R, Shapiro R, Taylor FR, Baker DP, Asahara T, Isner JM. The morphogen Sonic hedgehog is an

indirect angiogenic agent upregulating two families of angiogenic growth factors. *Nat Med.* 2001;7:706–711.
27. Renault MA, Chapouly C, Yao Q, Larrieu-Lahargue F, Vandierdonck S, Reynaud A, Petit M, Jaspard-Vinassa B, Belloc I, Traiffort E, Ruat M, Duplaa C, Couffinhal T, Desgranges C, Gadeau AP. Desert hedgehog promotes ischemia-induced angiogenesis by ensuring peripheral nerve survival. *Circ Res*. 2013;112:762–770. doi:10.1161/CIRCRESAHA.113.300871.
28. Queiroz KC, Bijlsma MF, Tio RA, Zeebregts CJ, Dunaeva M, Ferreira CV, Fuhler GM, Kuipers EJ, Alves MM, Rezaee F, Spek CA, Peppelenbosch MP. Dichotomy in Hedgehog signaling between human healthy vessel and atherosclerotic plaques. *Mol Med*. 2012;18:1122-1127. doi:10.2119/molmed.2011.00250.
29. Beckers L, Lutgens E, Heeneman S, Wang L, Burkly LC, Rousch MM, Davidson NO, Gijbels MJ, de Winther MP, Daemen MJ. Disruption of hedgehog signalling in ApoE -/- mice reduces plasma lipid levels, but increases atherosclerosis due to enhanced lipid uptake by macrophages. *J Pathol.* 2007;212:420–428.
30. Morris GE, Braund PS, Moore JS, Samani NJ, Codd V, Webb TR. Coronary Artery Disease-Associated LIPA Coding Variant rs1051338 Reduces Lysosomal Acid Lipase Levels and Activity in Lysosomes. *Arterioscler Thromb Vasc Biol*. 2017;37:1050-1057. doi: 10.1161/ATVBAHA.116.308734.
31. Taipale J, Chen JK, Cooper MK, Wang B, Mann RK, Milenkovic L, Scott MP, Beachy PA. Effects of oncogenic mutations in Smoothened and Patched can be reversed by cyclopamine. *Nature.* 2000;406:1005–1009.
32. Uhlén M, Fagerberg L, Hallström BM, Lindskog C, Oksvold P, Mardinoglu A, Sivertsson Å, Kampf C, Sjöstedt E, Asplund A, Olsson I, Edlund K, Lundberg E, Navani S, Szigyarto CA, Odeberg J, Djureinovic D, Takanen JO, Hober S, Alm T, Edqvist PH, Berling H, Tegel H, Mulder J, Rockberg J, Nilsson P, Schwenk JM, Hamsten M, von Feilitzen K, Forsberg M, Persson L, Johansson F, Zwahlen M, von Heijne G, Nielsen J, Pontén F. Proteomics. Tissue-based map of the human proteome. *Science.* 2015;347:1260419. doi:10.1126/science.1260419.
33. Chuang P-T, Kawcak T, Mcmahon AP. Feedback control of mammalian Hedgehog signaling by the Hedgehog- binding protein, Hip1, modulates Fgf signaling during branching morphogenesis of the lung. *Genes Dev*. 2003;17:342–347.
34. Wilk JB, Chen T-H, Gottlieb DJ, Walter RE, Nagle MW, Brandler BJ, Myers RH, Borecki IB, Silverman EK, Weiss ST, O'Connor GT. A genome-wide association study of pulmonary function measures in the Framingham Heart Study. *PLoS Genet*. 2009;5:e1000429. doi:10.1371/journal.pgen.1000429.
35. Pillai SG, Ge D, Zhu G, Kong X, Shianna KV, Need AC, Feng S, Hersh CP, Bakke P, Gulsvik A, Ruppert A, Lødrup Carlsen KC, Roses A, Anderson W, Rennard SI, Lomas DA, Silverman EK, Goldstein DB; ICGN Investigators.. A genome-wide association study in chronic obstructive pulmonary disease (COPD): identification of two major susceptibility loci. *PLoS Genet*. 2009;5:e1000421. doi:10.1371/journal.pgen.1000421.
36. Lao T, Jiang Z, Yun J, Qiu W, Guo F, Huang C, Mancini JD, Gupta K, Laucho-Contreras ME, Naing ZZC, Zhang L, Perrella MA, Owen CA, Silverman EK, Zhou X. Hhip haploinsufficiency sensitizes mice to age-related emphysema. *Proc Natl Acad Sci USA*. 2016;113:E4681-4687. doi:10.1073/pnas.1602342113.
37. Hohenester E, Sasaki T, Timpl R. Crystal structure of a scavenger receptor cysteine-rich domain sheds light on an ancient superfamily. Nat Struct Biol 1999;6:228–232. doi:10.1038/6669.
38. Jeong J, McMahon AP. Cholesterol modification of Hedgehog family proteins. *J Clin Invest*. 2002;110:591–596.

39. Passman JN, Dong XR, Wu S-P, Maguire CT, Hogan KA, Bautch VL, Majesky MW. A sonic hedgehog signaling domain in the arterial adventitia supports resident Sca1+ smooth muscle progenitor cells. *Proc Natl Acad Sci USA*. 2008;105:9349–9354. doi:10.1073/pnas.0711382105.
40. Morrow D, Cahill PA, Cullen JP, Liu W, Guha S, Sweeney C, Birney YA, Collins N, Walls D, Redmond EM. Sonic Hedgehog Induces Notch Target Gene Expression in Vascular Smooth Muscle Cells via VEGF-A. *Arterioscler Thromb Vasc Biol*. 2009;29:1112–1118. doi:10.1161/ATVBAHA.109.186890.
41. Redmond EM, Hamm K, Cullen JP, Hatch E, Cahill PA, Morrow D. Inhibition of patched-1 prevents injury-induced neointimal hyperplasia. *Arterioscler Thromb Vasc Biol* .2013;33:1960–1964. doi:10.1161/ATVBAHA.113.301843.
42. Briscoe J, Thérond PP. The mechanisms of Hedgehog signalling and its roles in development and disease. *Nat Rev Mol Cell Biol*. 2013;14:416-429. doi: 10.1038/nrm3598.
43. Araújo SJ. The Hedgehog Signalling Pathway in Cell Migration and Guidance: What We Have Learned from Drosophila melanogaster. *Cancers (Basel)*. 2015;7:2012-2022. doi: 10.3390/cancers7040873.
44. Fu JR, Liu WL, Zhou JF, Sun HY, Xu HZ, Luo L, Zhang H, Zhou YF. Sonic hedgehog protein promotes bone marrow-derived endothelial progenitor cell proliferation, migration and VEGF production via PI 3-kinase/Akt signaling pathways. *Acta Pharmacol Sin.* 2006;27:685–693.
45. Morrow D, Cahill PA, Sweeney C, Birney YA, Guha S, Collins N, Cummins PM, Murphy R, Walls D, Redmond EM. Biomechanical regulation of hedgehog signaling in vascular smooth muscle cells in vitro and in vivo. *Am J Physiol Cell Physiology*. 2007;292:C488-496.
46. Li F, Duman-Scheel M, Yang D, Du W, Zhang J, Zhao C, Qin L, Xin S. Sonic hedgehog signaling induces vascular smooth muscle cell proliferation via induction of the G1 cyclin-retinoblastoma axis. *Arterioscler Thromb Vasc Biol*. 2010;30:1787–1794. doi:10.1161/ATVBAHA.110.208520.
47. Wang G, Zhang Z, Xu Z, Yin H, Bai L, Ma Z, Decoster MA, Qian G, Wu G. Activation of the sonic hedgehog signaling controls human pulmonary arterial smooth muscle cell proliferation in response to hypoxia. *Biochim Biophys Acta*. 2010;1803:1359–1367. doi:10.1016/j.bbamcr.2010.09.002.
48. Lin L, Bu L, Cai C-L, Zhang X, Evans S. Isl1 is upstream of sonic hedgehog in a pathway required for cardiac morphogenesis. *Dev Biol*. 2006;295:756–763.
49. Sekulic A, Migden MR, Oro AE, Dirix L, Lewis KD, Hainsworth JD, Solomon JA, Yoo S, Arron ST, Friedlander PA, Marmur E, Rudin CM, Chang ALS, Low JA, Mackey HM, Yauch RL, Graham RA, Reddy JC, Hauschild A. Efficacy and safety of vismodegib in advanced basal-cell carcinoma. *N Engl J Med.* 2012;366:2171–2179. doi:10.1056/NEJMoa1113713.
50. Migden MR, Guminski A, Gutzmer R, Dirix L, Lewis KD, Combemale P, Herd RM, Kudchadkar R, Trefzer U, Gogov S, Pallaud C, Yi T, Mone M, Kaatz M, Loquai C, Stratigos AJ, Schulze HJ, Plummer R, Chang AL, Cornélis F, Lear JT, Sellami D, Dummer R. Treatment with two different doses of sonidegib in patients with locally advanced or metastatic basal cell carcinoma (BOLT): a multicentre, randomised, double-blind phase 2 trial. *Lancet Oncol*. 2015;16:716–728. doi:10.1016/S1470-2045(15)70100-2.

Figure Legends

Figure 1. HHIPL1 is a secreted interactor of SHH

(**A**) Representative western blot of HEK293 cell lysates and conditioned media following transfection of HHIPL1-FLAG plasmid. (**B** and **C**) Representative confocal images of HEK293 cells expressing HHIPL1-GFP (green) co-stained with DAPI (blue). Scale bars=10 μm. (**D**) Western blots, immunoblotted with anti-GFP and anti-FLAG antibodies, following transfection of HEK293 cells with HHIPL1-FLAG, SHH-GFP and immunoprecipitation with anti-GFP beads. (**E**) Gli-luciferase activity in SHH-LIGHT2 cells incubated with conditioned media from HEK293 cells transfected with SHH-GFP, HHIPL1-GFP or HHIP-FLAG or a mixture of SHH-GFP with HHIPL1-GFP or HHIPL-FLAG, n=4-5. Error bars represent mean ± sd. $^{**}P \leq 0.01$, $^{***}P \leq 0.001$, ns = non-significant.

Figure 2. HHIPL1 regulates human AoSMC migration and proliferation

(**A**) *HHIPL1* mRNA expression in human aortic smooth muscle cells (AoSMC), coronary artery endothelial cells (CAEC), peripheral blood mononuclear cells (PBMC) and macrophages (MP) relative to *36B4*. (**B**) *HHIPL1* mRNA expression relative to *RPLP0* in AoSMCs 24-72 hours post-transfection. (**C**) Migration rate of rate of human AoSMCs following siRNA transfection (left-panel) (n=3). Representative images of wound healing assay (right-panel). (**D**) Number of AoSMCs over 72 hours following siRNA knockdown. (**E**) Proportion of apoptotic cells 48 hours post-knockdown. (**F**) *GLI1* and *PTCH1* expression relative to *RPLP0* 48 hours after siRNA knockdown. (**G**) Representative western blot of GLI1 following siRNA knockdown. β-actin was used as a loading control.

Figure 3. *Hhipl1* expression in atherosclerotic plaques

(**A**) Representative immunohistochemical staining with anti-alpha smooth muscle Actin antibody (SMA), anti-Hhipl1 and MOMA-2 in aortic root lesions from 18 week old *Apoe*$^{-/-}$ mice fed western diet for 12 weeks. Upper panel scale bars = 500 μm. Lower panel scale bars = 200 μm. (**B**) Immunofluorescent staining of aortic root lesion with DAPI, SMA and anti-Hhipl1. Scale bars = 100 μm. (**C**) *Hhipl1* mRNA expression relative to *Rpl4* in the aortic arch of 6-48 week old *Apoe*$^{-/-}$ mice. n=3-6 mice per time-point. Error bars represent mean ± sd. *represent post-hoc comparisons with 6 week time-point. **$P \leq 0.01$, ***$P \leq 0.001$.

Figure 4. HHIPL1 regulates mouse AoSMCs migration and proliferation

(**A**) Migration rate of *Hhipl1*$^{-/-}$ and wild-type AoSMCs in a scratch wound assay over a period of 24 hours (n=4). Representative images are included in the right-hand panel. (**B**) Proliferation of *Hhipl1*$^{-/-}$ and wild-type AoSMCs over a period of 96 hours (n=4). * shown for significant post-hoc comparisons at 72 and 96 hours. (**C**) Proportion of apoptotic wild-type and *Hhipl1*$^{-/-}$ AoSMCs. (**D**) Gli-luciferase activity in SHH-LIGHT2 cells co-cultured with either wild-type or *Hhipl1*$^{-/-}$ AoSMCs, n=4. (**E**) *Gli1* and *Ptch1* mRNA expression relative to *Rplp0* in wild-type and *Hhipl1*$^{-/-}$ AoSMCs, n=5. Error bars represent mean ± sd. *$P \leq 0.05$, **$P \leq 0.01$, ***$P \leq 0.001$. (**F**) Western blot showing Gli1 expression in wild-type and knockout cells. β-actin was used as a loading control.

Figure 5. *Hhipl1* deficiency reduces atherosclerosis in *Hhipl1*$^{-/-}$; *Apoe*$^{-/-}$ and *Hhipl1*$^{-/-}$; *Ldlr*$^{-/-}$

(**A**) Representative Oil Red O stained (ORO) aortas from *Hhipl1*$^{+/+}$; *Ldlr*$^{-/-}$ and *Hhipl1*$^{-/-}$; *Ldlr*$^{-/-}$ mice. (**B**) Quantification of atherosclerosis in the aortas of mice of each genotype as a percentage of total aorta area (n=18 vs n=19). (**C**) Representative microphotographs of ORO

stained aortic root sections from *Hhipl1*$^{+/+}$*; Ldlr*$^{-/-}$ and *Hhipl1*$^{-/-}$*; Ldlr*$^{-/-}$ mice. (**D**) Aortic root lesion area (9 sections per mouse, n=6 per group). (**E**) ORO stained aortas from *Hhipl1*$^{+/+}$; *Apoe*$^{-/-}$ and *Hhipl1*$^{-/-}$; *Apoe*$^{-/-}$mice. (**F**) Quantification of atherosclerosis in the aortas of mice of each genotype (n=19 vs n=18). (**G**) ORO stained aortic roots from *Hhipl1*$^{+/+}$; *Apoe*$^{-/-}$ and *Hhipl1*$^{-/-}$; *Apoe*$^{-/-}$ mice. (**H**) Aortic root lesion area (9 sections per mouse, n=10 vs n=6). (**A** and **E**) scale bars=2mm. (**C** and **G**) scale bars=200 μm. Error bars represent mean ± CI. **P*≤0.05, ****P*≤ 0.001.

Figure 6. *Hhipl1* deficiency reduces smooth muscle cell content in *Hhipl1*$^{-/-}$*; Ldlr*$^{-/-}$ atherosclerotic lesions

Representative photomicrographs of atherosclerotic lesion components in *Hhipl1*$^{+/+}$*; Ldlr*$^{-/-}$ and *Hhipl1*$^{-/-}$*; Ldlr*$^{-/-}$ mice. (**A**) Oil red O (ORO) staining for lipids, (**C**) MOMA-2 staining for macrophages, (**E**) anti-alpha smooth muscle Actin (SMA) staining for smooth muscle cells and (**G**) Masson's Trichrome for collagen. Scale bars=200μm. The percentage content (average of 9 sections per animal) of (**B**) lipids, (**D**) macrophages, (**F**) smooth muscle cells and (**H**) collagen (n=6 per group). Error bars represent mean ± CI. ***P*≤ 0.01.

Figure 7. *Hhipl1* deficiency reduces smooth muscle cell content in *Hhipl1*$^{-/-}$*; Apoe*$^{-/-}$ atherosclerotic lesions

Representative photomicrographs of atherosclerotic lesion components in *Hhipl1*$^{+/+}$*; Apoe*$^{-/-}$ and *Hhipl1*$^{-/-}$*; Apoe*$^{-/-}$ mice. (**A**) Oil red O (ORO) staining for lipids, (**C**) MOMA-2 staining for macrophages, (**E**) anti-alpha smooth muscle Actin (SMA) staining for smooth muscle cells and (**G**) Masson's Trichrome for collagen. Scale bars=200μm. The percentage coverage (average of 9 sections per animal) of (**B**) lipids, (**D**) macrophages, (**F**) smooth muscle cells,

P=0.001, and (**H**) collagen (n=6-10 per group). Error bars represent mean ± CI. **P*≤ 0.05, ***P*≤ 0.01. Scale bars=200μm.

A

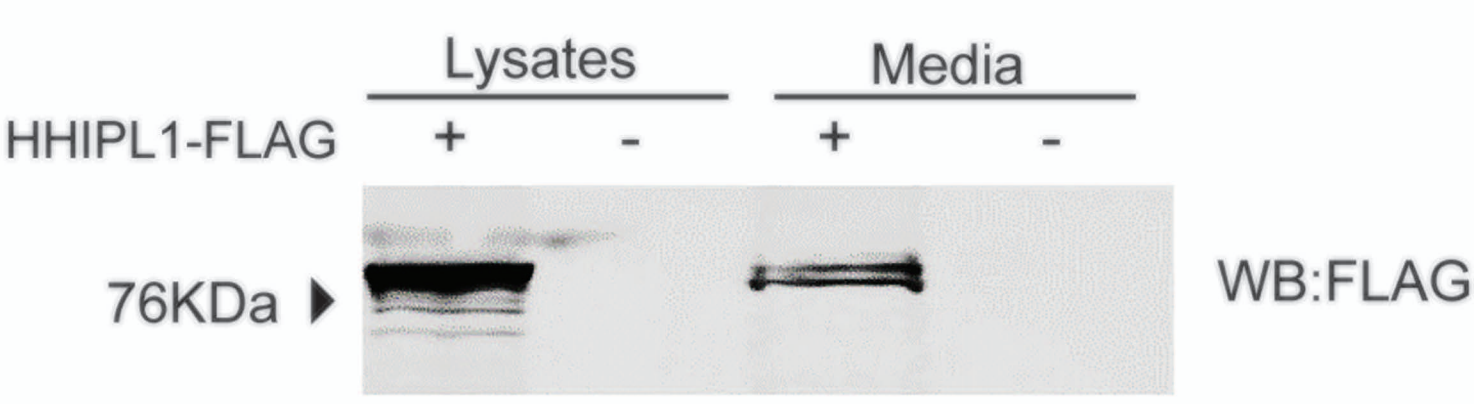

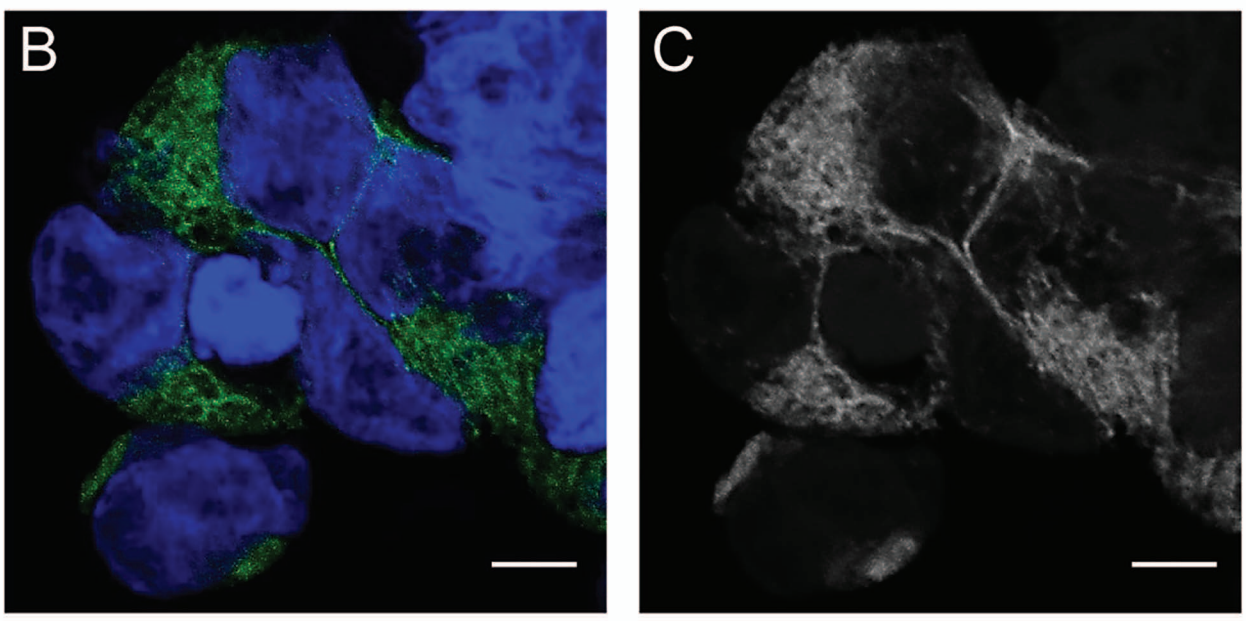

D